

Semi-flexible polymers with attractive interactions

R. Bundschuh^a, M. Lässig, and R. Lipowsky^b

MPI für Kolloid- und Grenzflächenforschung Am Mühlenberg, 14476 Golm, Germany

Received 15 December 1999 and Received in final form 19 May 2000

Abstract. The delocalization and unbinding transitions of two semi-flexible polymers which experience attractive interactions are studied by a variety of theoretical methods. In two-dimensional systems, one has to distinguish four different universality classes for the interaction potentials. In particular, the delocalization transitions from a potential well and the unbinding transitions from such a well in the presence of a hard wall exhibit distinct critical behavior governed by different critical exponents. In three-dimensional systems, we predict first-order transitions with a jump in the energy density but with critical or self-similar fluctuations leading to distribution functions with power law tails. The predicted critical behavior is confirmed numerically by transfer matrix calculations in two dimensions and by Monte Carlo simulations in three dimensions. This behavior should be accessible to experiments on biopolymers such as actin filaments or microtubuli.

PACS. 64.60.Fr Equilibrium properties near critical points, critical exponents – 61.41.+e Polymers, elastomers, and plastics – 05.40.-a Fluctuation phenomena, random processes, noise, and Brownian motion

1 Introduction

Semi-flexible polymers play an important role in many biomaterials [1] and biomimetic systems. In a physical description of their statistical properties the chemical details of these polymers can be summarized in a small set of parameters characterizing the individual features of a given polymer species. One important parameter is the bending stiffness. The latter quantity can be characterized by the persistence length, which is the length scale over which correlations in the orientation of single polymer segments decay. A polymer which is much longer than its persistence length behaves effectively as a flexible chain of loosely connected rigid segments, the size of which is set by the persistence length. This limit is well understood [2]. In some cases, the persistence length is quite large compared to atomic length scales. One example for such a semi-flexible polymer which behaves as a worm-like chain [3–5] is provided by double-stranded DNA which has a persistence length of the order of 50 nm. In general, the persistence length of a polymer is determined by several interactions between the monomers such as the stiffness of covalent bonds and the electrostatic repulsion between charged chain segments [6, 7].

If two semi-flexible polymers interact with each other via an attractive short-range interaction they can be bound together, because this is *energetically* favorable. On the other hand, the *entropy* of two bound polymers

fluctuating together is reduced compared to the situation where both polymers are separated and fluctuate independently of each other. This competition of energy and entropy leads to a phase transition at some critical temperature [8–10]. This transition is called the unbinding transition and can arise for all kinds of flexible or semi-flexible manifolds [9, 11]. In this article, we will classify and characterize the unbinding transitions of semi-flexible polymers in $1 + 1$ and $1 + 2$ dimensions.

The unbinding transition of semi-flexible polymers is driven by their thermally excited bending fluctuations. The latter fluctuations dominate as long as the corresponding correlation length is small compared to the persistence length. This regime which is studied below from a theoretical point of view is experimentally accessible for biopolymers such as actin filaments or microtubuli which have a large persistence length of the order of many micrometers [12–14].

The article is organized as follows: In Section 2 we discuss how the critical behavior of semi-flexible polymers can be characterized in general and especially at an unbinding transition. Section 3 then discusses the case of $1 + 1$ dimensional polymers, *i.e.*, of semi-flexible polymers confined to a two-dimensional system. All universality classes are determined which are needed to describe the unbinding transitions in $1 + 1$ dimensions and the critical exponents characterizing these transitions. These exponents are confirmed numerically. We also discuss how the unbinding transitions are modified by the presence of long-ranged interactions. In the last section we study the

^a *Current address:* UCSD, Physics Department, 9500 Gilman Drive, La Jolla, CA 92093-0319, USA.

^b e-mail: lipowsky@mpikg-golm.mpg.de

unbinding transition in 1+2 dimensions, *i.e.*, the behavior of semi-flexible polymers in three-dimensional systems.

2 Delocalization and unbinding transitions

2.1 Statistical weight and partition function

As already mentioned in the introduction, we will study semi-flexible polymers on length scales which are small compared to their persistence length. These polymers then undergo bending fluctuations governed by their bending stiffness or rigidity. We describe their conformations, which have no overhangs, by the parameterization $(t, z(t))$ where the longitudinal coordinate t satisfies $0 \leq t \leq L_{\parallel}$ and the transverse coordinate $z(t)$ is a d_{\perp} -dimensional displacement field. For $d_{\perp} = 2$, one has the usual physical situation of a polymer embedded in three dimensions but the case $d_{\perp} = 1$ can also be realized if the fluctuations of the polymers are restricted in one direction by the experimental setup. The energy functional of the polymer is given by

$$\mathcal{H}_0\{z\} \equiv \int_0^{L_{\parallel}} dt \frac{\kappa}{2} \left(\frac{d^2 z}{dt^2} \right)^2, \quad (1)$$

where κ is the bending stiffness. It is related to the persistence length l_p by $l_p = 2\kappa/T$ with temperature T in energy units. For a compact description of the semi-flexible polymer it is convenient to absorb these phenomenological parameters into rescaled quantities. Thus, we will use the rescaled displacement field

$$\ell \equiv \left(\frac{\kappa}{T} \right)^{1/2} z \quad (2)$$

for the description of the polymer conformations. Its dimensionless energy functional is

$$\bar{\mathcal{H}}_0\{\ell\} \equiv \frac{\mathcal{H}_0}{T} = \int_0^{L_{\parallel}} dt \frac{1}{2} \left(\frac{d^2 \ell}{dt^2} \right)^2. \quad (3)$$

The partition function of the polymer with boundary conditions $\ell(t=0) = \ell_0$ and $d\ell/dt|_{t=0} = v_0$ at one end and $\ell(t=L_{\parallel}) = \ell_1$ and $d\ell/dt|_{t=L_{\parallel}} = v_1$ at the other end has the path integral form

$$Z_{L_{\parallel}}(\ell_1, v_1 | \ell_0, v_0) = \int \mathcal{D}\{\ell\} \exp(-\bar{\mathcal{H}}_0\{\ell\})$$

and can be easily calculated [10] with the result

$$Z_{L_{\parallel}}(\ell_1, v_1 | \ell_0, v_0) = \left(\frac{\sqrt{3}}{\pi L_{\parallel}^2} \right)^{d_{\perp}} \times \exp[-6\Omega(\ell_1, v_1 | \ell_0, v_0)/L_{\parallel}^3], \quad (4)$$

with

$$\begin{aligned} \Omega(\ell_1, v_1 | \ell_0, v_0) &\equiv (\ell_1 - \ell_0 - v_0 L_{\parallel})^2 \\ &\quad - L_{\parallel}(\ell_1 - \ell_0 - v_0 L_{\parallel})(v_1 - v_0) \\ &\quad + \frac{L_{\parallel}^2}{3}(v_1 - v_0)^2. \end{aligned} \quad (5)$$

We now consider two semi-flexible polymers with mutual interactions. Their behavior can be fully described in terms of a freely fluctuating displacement field for the ‘‘center of mass’’ motion and another displacement field which describes the separation of the two polymers. In the following we will therefore focus on the behavior of the separation field only, again denoted by ℓ . The interaction between the two polymers is now equivalent to the interaction of one polymer with a localized external potential at $\ell = 0$.

We will distinguish several types of interactions: i) The interaction of two polymers which cannot penetrate each other is described by a repulsive hard wall interaction; ii) Two polymers which attract each other by intermolecular forces experience a combined interaction potential which consists both of a repulsive hard wall interaction and of an attractive potential well; and iii) It is also instructive to study interactions with an attractive potential well but without a hard wall interaction even though such a potential is difficult to realize experimentally.

As one varies a parameter such as the temperature, two polymers which attract each other may undergo an unbinding transition from a bound state at low temperatures to an unbound state at high temperatures. Likewise, a polymer which experiences an attractive potential well may undergo a delocalization transition from a localized to a delocalized state.

In general, one must distinguish several universality classes for these interaction potentials which depend on the decay of these potentials for large separation ℓ . Below, we will explicitly discuss short-ranged potentials which have a finite potential range. However, these potentials belong to a rather large universality class which contains *all* potentials decaying faster than $|\ell|^{-2/3}$ for large separation ℓ [9, 10]. Therefore, the critical behavior obtained here for the short-ranged case applies in fact to all physically relevant interactions.

2.2 Scaling behavior

First, let us again consider the free polymer of length L_{\parallel} with the statistical weight as given by (3) and the partition function (4). The latter function may be rewritten in the scaling form

$$Z_{L_{\parallel}}(\ell, v | 0, 0) = L_{\parallel}^{-2d_{\perp}} \Xi(|\ell| L_{\parallel}^{-3/2}, v L_{\parallel}^{-1/2}), \quad (6)$$

with the scaling function

$$\Xi(\bar{\ell}, \bar{v}) \equiv \left(\frac{\sqrt{3}}{\pi} \right)^{d_{\perp}} \exp[-6\bar{\ell}^2 + 6\bar{\ell}\bar{v} - 2\bar{v}^2], \quad (7)$$

which depends on the rescaled displacement $\bar{\ell} \equiv |\ell| L_{\parallel}^{-3/2}$ and the rescaled orientation $\bar{v} \equiv v L_{\parallel}^{-1/2}$. These rescaled quantities arise from the typical fluctuations of the polymer. Indeed, using the statistical weight (3), one easily finds that $\langle \ell^2 \rangle \sim L_{\parallel}^3$ and $\langle v^2 \rangle = \langle (d\ell/dt)^2 \rangle \sim L_{\parallel}$. Thus, the typical displacements are governed by the length scale

$L_{\perp} \equiv \langle \ell^2 \rangle^{1/2} \sim L_{\parallel}^{3/2}$ and the typical orientations are of the order of $\langle (d\ell/dt)^2 \rangle^{1/2} \sim L_{\parallel}^{1/2} = L_{\perp}/L_{\parallel}$.

It will be convenient to rewrite the scaling form (6) in terms of $\bar{\ell} = |\ell|L_{\parallel}^{-3/2}$ and the L_{\parallel} -independent ratio $\bar{v}/\bar{\ell}^{1/3} = v|\ell|^{-1/3}$ which leads to

$$Z_{L_{\parallel}}(\ell, v|0, 0) = L_{\parallel}^{-2d_{\perp}} \Omega\left(|\ell|L_{\parallel}^{-3/2}, v|\ell|^{-1/3}\right), \quad (8)$$

with

$$\Omega(\bar{\ell}, \bar{v}) \equiv \Xi(\bar{\ell}, \bar{v}|\ell|^{1/3}) \quad (9)$$

for the free polymer.

Next, let us introduce an interaction potential which the polymer experiences at small values of $|\ell|$. Such a potential will, in general, change the form of the partition function. However, since the potentials considered here are localized at $|\ell| = 0$ and are (effectively) short-ranged, the large scale excursions of the polymer will be unaffected by these potentials. Thus, its typical displacements are again governed by the length scale $L_{\perp} \sim L_{\parallel}^{3/2}$, and its typical orientations are again of the order of $\langle (d\ell/dt)^2 \rangle^{1/2} \sim L_{\perp}/L_{\parallel} = L_{\parallel}^{1/2}$ for large L_{\parallel} . On the other hand, these interaction potentials are expected to change the short-distance behavior of the partition function at small values of $|\ell|$. Therefore, an interaction potential localized at $|\ell| = 0$ should lead to the generalized scaling form

$$Z_{L_{\parallel}}(\ell, v|0, 0) = |\ell|^{\theta/2} L_{\parallel}^{-x} \Omega\left(|\ell|L_{\parallel}^{-3/2}, v|\ell|^{-1/3}\right) \quad (10)$$

for the restricted partition function $Z_{L_{\parallel}}$. An equivalent scaling form has been proposed previously for the (1+1)-dimensional case [8, 10]. The two critical exponents θ and x are defined by the regularity condition $\Omega(0, 0) = \text{const}$ for the scaling function Ω at small arguments.

The exponents x and θ in (10) are not independent but satisfy a scaling relation as in $d = 1 + 1$ [10]. This scaling relation follows from the property that the partition function Z_L satisfies a Chapman-Kolmogorov equation in which $Z_{L+M}(\ell_2, v_2|\ell_0, v_0)$ is expressed as the convolution of $Z_L(\ell_2, v_2|\ell_1, v_1)$ and $Z_M(\ell_1, v_1|\ell_0, v_0)$. Using this property in $d = 1 + d_{\perp}$, one obtains the scaling relation

$$x = 2d_{\perp} + 3\theta/2, \quad (11)$$

which can be easily verified for the free system with $x = x_0 = 2d_{\perp}$ and $\theta = \theta_0 = 0$ as follows from (6) and (8).

The exponent θ describes the short-distance behavior of several observables and is therefore particularly suited for characterizing the critical behavior at the delocalization or unbinding transitions. In order to determine this critical behavior, we vary a parameter, typically the rescaled potential strength, and study how the polymer evolves from a strongly bound state to a weakly bound one. In a bound state, the fluctuations of the polymer are confined and are governed by a longitudinal correlation

length, ξ_{\parallel} . This implies that the restricted partition function still has the scaling form as given by (10) *provided* one has $L_{\parallel} \ll \xi_{\parallel}$. On the other hand, if the system size L_{\parallel} satisfies $L_{\parallel} \gg \xi_{\parallel}$, the restricted partition function attains the asymptotic form

$$Z_{L_{\parallel}}(\ell, v|0, 0) \approx |\ell|^{\theta/2} \xi_{\parallel}^{-x} \Omega\left(|\ell|\xi_{\parallel}^{-3/2}, v|\ell|^{-1/3}\right) \quad (12)$$

as follows from (10) with L_{\parallel} replaced by ξ_{\parallel} .

Now, consider the probability distribution $\psi(\ell, v)$ in such a stationary state which describes the probability to find the end of the polymer at a distance ℓ from the origin with orientation v . This distribution is obtained by normalization of the restricted partition function and, thus, given by

$$\psi(\ell, v) = \frac{Z_{L_{\parallel}}(\ell, v|0, 0)}{\int_0^{\infty} d\ell \int_{-\infty}^{\infty} dv Z_{L_{\parallel}}(\ell, v|0, 0)}, \quad (13)$$

where $Z_{L_{\parallel}}(\ell, v|0, 0)$ has the L_{\parallel} -independent scaling form (12) in the limit of large $L_{\parallel} \gg \xi_{\parallel}$.

It now follows from the relations (13) and (12) that the form of the probability distribution $\psi(\ell, v)$ for small ℓ is completely characterized by the exponent θ . This gives us the behavior of several observables at small separations from the potential well. First, consider the behaviour in $d_{\perp} = 1$. The probability $P_{\text{tan}}^{(e)}(\ell)$ to find the end of the polymer at the distance $|\ell|$ with an orientation parallel to the potential well scales as

$$P_{\text{tan}}^{(e)}(\ell) \equiv \psi(\ell, 0) \sim |\ell|^{\theta/2}. \quad (14)$$

Likewise, the probability to find the polymer at a certain distance $|\ell|$ with any orientation v is given by

$$P^{(e)}(\ell) \equiv \int_{-\infty}^{\infty} dv \psi(\ell, v) \sim |\ell|^{(\theta/2)+(1/3)}. \quad (15)$$

If we consider segments in the middle of the polymer, we have to take into account the statistics of the two pieces of the polymer which connect the segment in the middle with both ends. It follows from the transfer matrix formalism that the probability to find a segment in the middle of the polymer at a given distance with an orientation parallel to the potential well is given by $\psi(\ell, 0)^2$ and, thus, scales as

$$P_{\text{tan}}(\ell) \equiv [\psi(\ell, 0)]^2 \sim |\ell|^{\theta}. \quad (16)$$

If we do not resolve the orientation of the segment, we again have to integrate over the orientations and get the probability

$$P(\ell) \equiv \int_{-\infty}^{\infty} dv \psi(\ell, v)\psi(\ell, -v) \sim |\ell|^{\theta+(1/3)} \quad (17)$$

to find the segment at a given distance $|\ell|$ with an arbitrary orientation. For $d_{\perp} > 1$, the radial distributions

$P(|\ell|)$ are obtained multiplying (14) and (16) by $|\ell|^{d_\perp-1}$, but (15) and (17) by $|\ell|^{4(d_\perp-1)/3}$.

At this point, let us summarize the scaling properties discussed above. First, without any interaction potential at $\ell = 0$, the semi-flexible polymer makes wide excursions from this reference line in order to increase its configurational entropy. This state is characterized by the exponents $\theta = \theta_0 = 0$ and $x = x_0 = 2d_\perp$. If we now add a short-ranged interaction potential which is localized at $|\ell| = 0$, we will change the scaling properties of the polymer fluctuations for small values of $|\ell|$. If this potential is attractive, we can induce a phase transition from the free state to a state in which the polymer is bound to the potential well (or the two polymers are bound together.) At this delocalization (or unbinding) transition, the system is again scale invariant and therefore characterized by exponents $\theta = \theta^*$ and $x = x^*$ which are, in general, different from the exponents θ_0 and x_0 for the free polymer.

2.3 Relation with directed lines or strings

The systematic field-theoretic study of delocalization or unbinding transitions of semi-flexible polymers in references [15,16] shows that these transitions are intimately related to the corresponding transitions of directed lines or strings. This relation becomes apparent if one compares the perturbation series for the partition functions as appropriate in both cases. In the absence of the short-ranged attraction, the partition function Z of the semi-flexible polymer exhibits the scaling behavior $Z_t(0,0|0,0) \sim t^{-x_0}$ as in (6). As explained in the appendix, the perturbation series arising from the short-ranged attraction can be formally mapped, term by term, onto the corresponding perturbation series for the delocalization or unbinding transitions of directed lines in $1 + d'_\perp$ dimensions with $d'_\perp = 2x_0$.

If one ignores the formal character of these perturbation series, one also concludes that the critical exponent $x = x^*$ at the delocalization or unbinding transition of the semi-flexible polymer is identical to the contact exponent $\zeta_2 = \zeta_2^*$ which governs the probability of local contacts between the directed line or string and the potential well at the transitions. Note that the critical exponent x determines the decay of the probability for *tangential* contacts of the semi-flexible polymer, *i.e.*, for local contacts with orientation $v = 0$. In contrast, the exponent ζ_2 governs the probability for all local contacts of directed lines or strings.

If the semi-flexible polymer is “completely free” in the absence of the short-ranged attraction, *i.e.*, if it does not experience any repulsive wall or constraint, one has $x_0 = 2d_\perp$ as follows from (4). In this case, the short-ranged attraction leads to a delocalization transition from a potential well (or penetrable defect line). The perturbative mapping then implies that this transition belongs to the same universality class as the delocalization transition of a directed line or string in $1 + d'_\perp$ dimensions with $d'_\perp = 4d_\perp$. If the semi-flexible polymer is subject to repulsive or impenetrable walls, the critical exponent x_0 should

be increased which implies the inequality $x_0 \geq 2d_\perp$ and, thus, $d'_\perp \geq 4d_\perp$.

The critical behavior of directed lines or strings can be calculated exactly using analytical transfer matrix methods [17]. One then finds that the contact exponent ζ_2^* has the value $\zeta_2^* = 2 - d'_\perp/2$ for $d'_\perp \geq 2$. The latter inequality is fulfilled in the present context as long as $d_\perp \geq 1/2$ as will be assumed here. Since $x^* = \zeta_2^*$ and $d'_\perp = 2x_0$ as mentioned, one obtains the scaling relation

$$x^* = 2 - d'_\perp/2 = 2 - x_0. \quad (18)$$

In fact, it has been previously shown for directed lines or strings, that the contact exponents $\zeta_2 = \zeta_2^*$ at the transition and $\zeta_2 = \zeta_{2,0}$ as appropriate for the delocalized or unbound state satisfy $\zeta_2^* + \zeta_{2,0} = 2$ in all dimensions d'_\perp . From the latter equality, one immediately obtains the scaling relation $x^* + x_0 = 2$ as in (18) if one identifies $x = x(d_\perp)$ with $\zeta_2 = \zeta_2(d'_\perp)$ both at the transition and for the unbound state. The latter property should apply to *any* mapping $d'_\perp = d'_\perp(d_\perp)$ between the critical behavior of the semi-flexible polymer and the corresponding behavior of the directed line or string since this mapping cannot depend on the strength of the short-ranged attraction.

Using the two relations (11) and (18), one also obtains

$$\theta^* = \frac{2}{3}(x^* - 2d_\perp) = \frac{2}{3}(2 - 2d_\perp - x_0). \quad (19)$$

Note that x^* changes sign at $d'_\perp = 4$. For $d'_\perp > 4$, one enters the so-called subregime (C) which exhibits unusual scaling properties [17]: in this latter subregime, the delocalization or unbinding transitions are discontinuous but observables such as those defined by (14)–(17) still exhibit nontrivial scaling properties.

3 Semi-flexible polymers in 2-dimensional systems

3.1 Universality classes for the strong fluctuation regime

In this section, we will study semi-flexible polymers in 2-dimensional systems, *i.e.*, for $d_\perp = 1$. Examples are provided by polymers which are confined to thin slabs. Several cases must be distinguished. In the context of two semi-flexible polymers with short-range attractions, these polymers can either cross each other or feel a hard core repulsion which prevents such crossings. In terms of the separation coordinate ℓ , the hard core repulsion corresponds to a hard wall potential at zero separation $\ell = 0$. Thus four different cases will be considered: i) Two semi-flexible polymers, which cannot cross each other, ii) two freely fluctuating semi-flexible polymers without any restrictions, iii) two semi-flexible polymers with an attractive short-ranged interaction, which cannot cross each other, and iv) two semi-flexible polymers, which feel an attractive short-range interaction but may cross each other. The corresponding interaction potentials $V(\ell)$ are displayed in

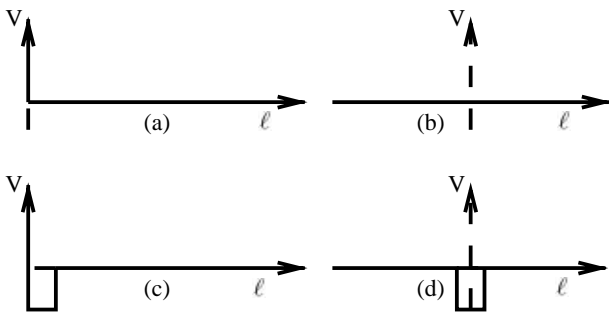


Fig. 1. Prototypes of interaction potentials $V(\ell)$ which belong to four different universality classes for the critical behavior of semi-flexible polymers in $1+1$ dimensions. As explained in the text, the associated fixed points are: (a) hard wall; (b) Gaussian; (c) unbinding transition; and (d) delocalization transition.

Figure 1. These four potentials represent four different universality classes, which, in the framework of the renormalization group, correspond to different fixed points of the renormalization group flow.

Each of these universality classes is characterized by specific values for the critical exponents x and θ which will now be determined. The calculation of the freely fluctuating polymer is trivial; from (4) we immediately read off the values $x_0 = 2$ and $\theta_0 = 0$. According to (18) and (19), this implies $x^* = 0$ and $\theta^* = -4/3$ at the corresponding delocalization transition which belongs to the prototype potential as shown in Figure 1(d).

With a hard wall but without a short-range interaction the problem can also be solved analytically [18] and one gets $x_0 = 5/2$ and $\theta_0 = 1/3$. The scaling relation (19) then leads to $\theta^* = -5/3$ at the unbinding transition in the presence of a hard wall which belongs to the prototype potential in Figure 1(c). The transition will be discontinuous. This unbinding transition in the presence of a hard core repulsion has already been studied semi-numerically in [10] with the result $\theta^* = -5/3$.

Thus, the critical behavior of semi-flexible polymers is governed by four different universality classes. This has to be compared with the behavior of thermally excited strings [19–21] and of strings in a random potential [22–26] for which one finds two and six different universality classes, respectively.

3.2 Numerical method

In order to test the theoretical predictions, extensive transfer matrix calculations have been performed numerically in $d = 1 + 1$. By this method the path integral

$$Z_{L_{\parallel}}(\ell_1, v_1 | \ell_0, v_0) = \int \mathcal{D}\{\ell\} \exp \left[- \int_0^{L_{\parallel}} dt \frac{1}{2} \left(\frac{d^2 \ell}{dt^2} \right)^2 + V \left(\ell, \frac{d\ell}{dt} \right) \right] \quad (20)$$

for the partition function is explicitly calculated. For this purpose, the time coordinate along the polymer is discretized into integer multiples of the time interval Δt .

A discretization of the position ℓ of the semi-flexible polymer into integer multiples of some length scale $\Delta \ell$ then implies that the possible velocities are integer multiples of $\Delta \ell / \Delta t$. The number of possible positions and velocities is made finite by choosing appropriate boundary conditions and allowing only the positions $-L_{\perp} \Delta \ell / 2, \dots, L_{\perp} \Delta \ell / 2$ and the velocities $-L_v \Delta \ell / 2 \Delta t, \dots, L_v \Delta \ell / 2 \Delta t$. This introduces two finite-size scales L_{\perp} and L_v . However, these two scales are not independent of each other. Since the roughness exponent ζ of a semi-flexible polymer is $\zeta = 3/2$, *i.e.*, the width of typical excursions of a semi-flexible polymer grows as the $3/2$ power of the length of the polymer, the velocities of a semi-flexible polymer which is restricted to a width of L_{\perp} in position space will only grow up to about $L_{\perp}^{(\zeta-1)/\zeta} = L_{\perp}^{1/3}$. We will always choose the large-scale cutoff L_v in velocity space sufficiently large compared to this value. In this way we ensure that the partition function does not change significantly if L_v is further increased. Thus, L_{\perp} is the only relevant finite-size scale.

For fixed initial conditions (ℓ_0, v_0) and each time $k \Delta t$ the restricted partition function

$$q_k(n, m) \equiv Z_{k \Delta t} \left(n \Delta \ell, m \frac{\Delta \ell}{\Delta t} \middle| \ell_0, v_0 \right), \quad (21)$$

with $n = -L_{\perp}/2, \dots, L_{\perp}/2$ and $m = -L_v/2, \dots, L_v/2$ is a vector of $L_{\perp} L_v$ entries. The Markov property

$$q_{k+1}(n, m) = \sum_{n'=-L_{\perp}/2}^{L_{\perp}/2} \sum_{m'=-L_v/2}^{L_v/2} z(n, m | n', m') q_k(n', m') \quad (22)$$

of the partition function allows an iterative calculation of the restricted partition function via the short time propagator

$$z(n, m | n', m') \equiv \frac{(\Delta \ell)^2}{\Delta t} Z_{\Delta t} \times \left(n \Delta \ell, m \frac{\Delta \ell}{\Delta t} \middle| n' \Delta \ell, m' \frac{\Delta \ell}{\Delta t} \right). \quad (23)$$

Ignoring global prefactors, which affect only the normalization, we approximate the path integral defining the short time propagator by its value along the “classical path”, *i.e.*,

$$z(n, m | n', m') \sim \exp \left[- \int_0^{\Delta t} dt \frac{1}{2} \left(\frac{d^2 \ell_{cl}(t)}{dt^2} \right)^2 \right] \times \exp \left[- \int_0^{\Delta t} dt V \left(\ell_{cl}(t), \frac{d\ell_{cl}(t)}{dt} \right) \right], \quad (24)$$

where $\ell_{cl}(t)$ is the classical path with the boundary conditions $\ell_{cl}(0) = n \Delta \ell$, $\frac{d\ell_{cl}}{dt}|_{t=0} = m \Delta \ell / \Delta t$, $\ell_{cl}(\Delta t) = n' \Delta \ell$, and $\frac{d\ell_{cl}}{dt}|_{t=\Delta t} = m' \Delta \ell / \Delta t$. Since $d^4 \ell_{cl} / dt^4 = 0$ is the classical equation of motion corresponding to (3), the classical path is a polynomial of third degree. Inserting the classical path into the first exponential in (24) gives the free

propagator as shown in (4) with L_{\parallel} replaced by Δt , *i.e.*, up to a normalization factor

$$z(n, m|n', m') \sim \exp \left\{ -\frac{6(\Delta\ell)^2}{(\Delta t)^3} \left[(n' - n - m)(n' - n - m') + \frac{(m' - m)^2}{3} \right] \right\} \times \exp \left[-\int_0^{\Delta t} dt V \left(\ell_{\text{cl}}(t), \frac{d\ell_{\text{cl}}(t)}{dt} \right) \right]. \quad (25)$$

From (25) it is clear that the largest contribution to the short time propagator $z(n, m|n', m')$ comes from the elements with $m' = m$ and $n' = n + m$. In order to keep the computer time within reasonable limits, we use the ‘‘RSOS’’ condition that we disallow any transitions for which the argument of the first exponential in (25) is smaller than -10 . These transitions are naturally suppressed by a factor of e^{-10} compared to the most probable transition. Thus, the choice of the discretization which determines the factor $(\Delta\ell)^2/(\Delta t)^3$, also determines how many points (n', m') in the neighborhood of $(n + m, m)$ can be reached by allowed transitions from (n, m) . By comparison with the analytically available solution for a semi-flexible polymer in a harmonic potential for different values of the discretization units, the choice of $(\Delta\ell)^2/(\Delta t)^3 = 1$ leading to the 7 allowed points $(n + m, m)$, $(n + m, m + 1)$, $(n + m, m - 1)$, $(n + m + 1, m)$, $(n + m + 1, m + 1)$, $(n + m - 1, m)$ and $(n + m - 1, m - 1)$ has been selected as a good compromise between numerical accuracy and computing time requirements.

In the case of directed lines or strings it is possible to replace the integral in the second exponential of (25) by the value of the potential at time Δt . This approximation is, however, not appropriate in the case of semi-flexible polymers. Indeed, the semi-flexible polymer can make transitions between two distant positions in one time step if its velocity is large. In the case of a spatially localized potential—such as the attractive short-range potentials considered here—the polymer can then jump over the potential in one time step without noticing the possible energy gain arising from the potential. Therefore, the integrals in the second exponential in (25) have been explicitly calculated via Monte Carlo integration along the classical path for every allowed combination (n, m, n', m') before the iteration step as given by (22) has been performed.

The short-ranged potential used here has been chosen to have a width ℓ_V of one discretization unit $\ell_V \equiv \Delta\ell$ symmetrically around the origin and is given by

$$V(\ell, v) = V_{\delta}(\ell) \equiv \begin{cases} \frac{g}{\Delta t}, & |\ell| \leq \ell_V, \\ 0, & |\ell| > \ell_V, \end{cases} \quad (26)$$

where $g < 0$ measures the strength of the attraction. In the presence of a hard wall, the potential used in the transfer-matrix calculations has the functional form

$$V(\ell, v) = V_{\text{w}}(\ell) \equiv \begin{cases} \infty, & \ell < 0, \\ \frac{g}{\Delta t}, & 0 \leq \ell \leq \ell_V, \\ 0, & \ell > \ell_V. \end{cases} \quad (27)$$

In physical units, the potential well has the strength

$$u = T \left(\frac{T}{\kappa} \right)^{1/3} z_V^{-2/3} g \quad (28)$$

and the potential width $z_V \equiv (T/\kappa)^{1/2} \ell_V = (T/\kappa)^{1/2} \Delta\ell$.

After the relation (22) has been iterated for a sufficient number of times, the obtained restricted partition function becomes, after normalization, the stationary distribution $\psi(\ell, v)$ for the positions and slopes of the end of the semi-flexible polymer. Convergence toward a stationary state is monitored by direct comparison of distributions which are several hundred time steps apart. For the largest systems used with $L_{\perp} = 10240$ and $L_v = 111$ close to the unbinding transition, up to $L_{\parallel} = 3000$ iterations were necessary in order to reach the stationary state. This amounts to a computing time on the order of 3 hours on an SGI or HP work station for one set of parameters.

Once the stationary distribution $\psi(\ell, v)$ has been obtained, the small- ℓ behavior of the four distributions (14)–(17) has been measured independently at the delocalization or unbinding transition. The position of the transition has been determined in two different ways. On the one hand, the quantity $\sigma(g, L_{\perp}) \equiv \langle \ell^2 \rangle_{g, L_{\perp}} / L_{\perp}^2$ has been measured as a function of the system size L_{\perp} and of the strength g of the attractive short-ranged potential. In the localized phase, this quantity is close to zero whereas it approaches a finite value in the delocalized phase. Plotting σ as a function of g for different L_{\perp} shows that it becomes independent of L_{\perp} for one specific value of g which we identify as the critical attraction strength $g = g_u$ for the transition. On the other hand, direct inspection of the distribution $\psi(\ell, 0)$ shows that this distribution decays exponentially for large separations ℓ provided $g = -|g|$ is sufficiently attractive but is cut off by the finite system size for sufficiently small values of $|g|$. This distinct behavior gives another estimate of the critical attraction strength g_u . Both estimates become more accurate with increasing system size L_{\perp} . The uncertainty in the value of the critical attraction strength g_u is mainly responsible for the errors in the measured exponents at the transition, see the discussion below.

3.3 Numerical results for the strong fluctuation regime

Using the methods described in the last section, the probability $P_{\text{tan}}(\ell)$ as given by (16), *i.e.*, the probability to find the two polymers tangential to each other at a given distance ℓ , has been measured for the four prototype potentials shown in Figure 1. The numerical data are displayed in Figure 2. Inspection of this figure shows that the numerical values for the critical exponent θ are in fair agreement with the theoretical predictions we obtained in Section 3.1.

We now focus on potentials $V = V_{\delta}$ as described by equation (26) which have a symmetric potential well but no hard wall, see Figure 1(d). First, we determined the critical attraction strength $g = g_u$ using the two different

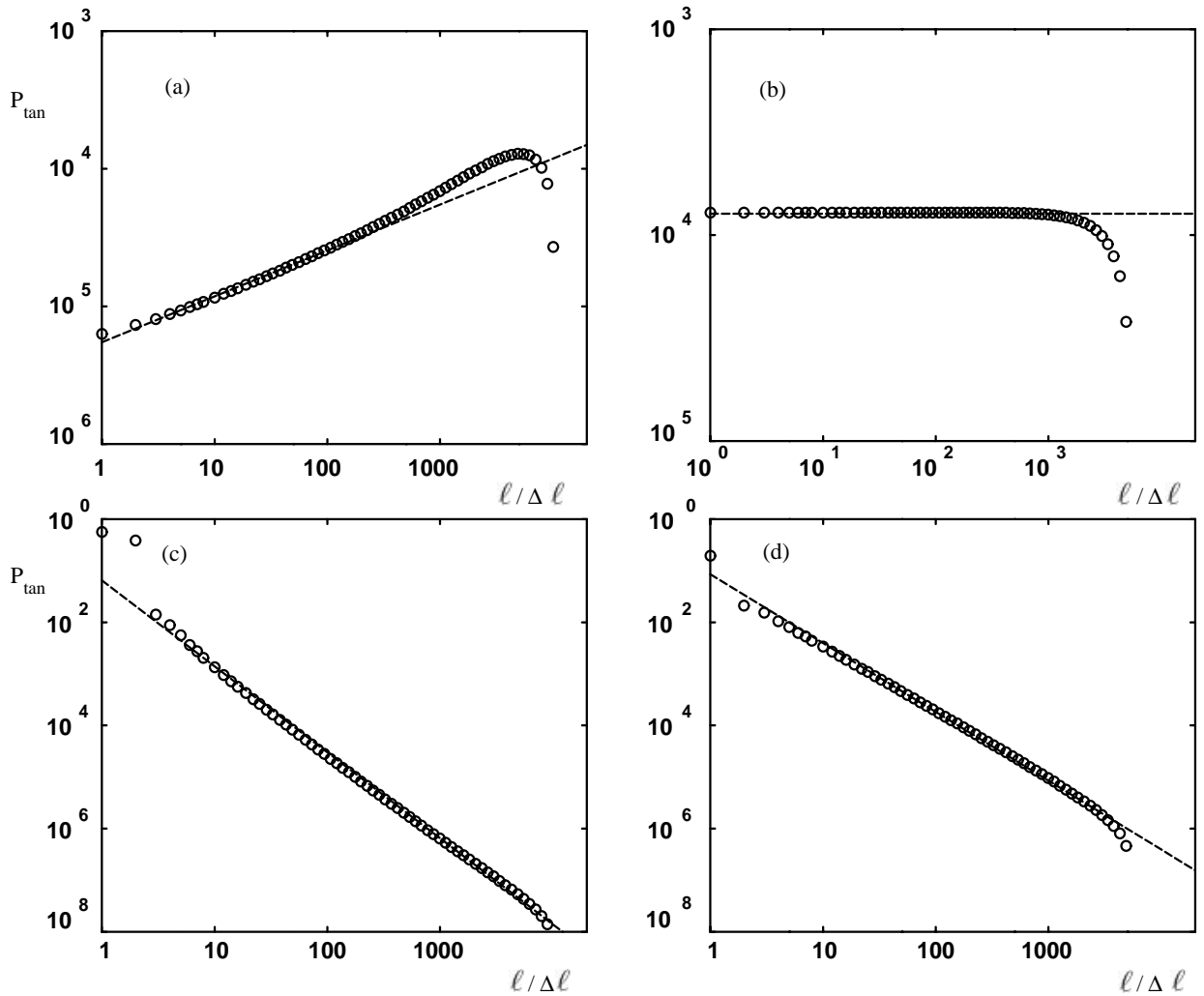


Fig. 2. Double logarithmic plots of the probability distribution $P_{\text{tan}}(\ell)$ to find the two polymers at a distance ℓ and parallel to each other. The four plots correspond to the four potentials shown in Figure 1. The dashed lines are the predicted power laws ℓ^θ with (a) $\theta = 1/3$, (b) $\theta = 0$, (c) $\theta = -5/3$, and (d) $\theta = -4/3$. The deviations of the data from the power law behavior at large separations ℓ arise from finite-size corrections.

methods described in Section 3.2 above. Both methods lead to the same estimate given by $g_u = -0.398 \pm 0.002$.

At the critical value $g = g_u$, the four probability distributions described by (14)–(17) are governed by the critical exponent $\theta = \theta^*$. From the numerical data for these different distributions, we have obtained four numerical estimates for θ^* : i) The probability $P_{\text{tan}}^{(e)}$ for the polymer end to be at distance $|\ell|$ with a tangential orientation parallel to the potential well is predicted to scale as $P_{\text{tan}}^{(e)} \sim |\ell|^{\theta/2}$. A double-logarithmic plot of the data for this distribution leads to the estimate $\theta^*/2 = -0.64 \pm 0.05$ and, thus, $\theta^* = -1.28 \pm 0.10$; ii) The probability $P^{(e)}(\ell)$ for the polymer end to be at distance $|\ell|$ (irrespective of its orientations) should scale as $P^{(e)}(\ell) \sim |\ell|^{\theta/2+1/3}$. The corresponding data lead to $\theta^*/2+1/3 = -0.35 \pm 0.04$ and, thus, to $\theta^* = -1.37 \pm 0.08$; iii) The probability $P_{\text{tan}}(\ell)$ for a polymer segment which is located in the middle of the polymer should behave as $P_{\text{tan}}(\ell) \sim |\ell|^\theta$. From the data

for this quantity, we find $\theta^* = -1.26 \pm 0.09$; and iv) The probability $P(\ell)$ for a polymer segment in the middle of the polymer is predicted to behave as $P(\ell) \sim |\ell|^{\theta+1/3}$ and the data analysis now gives $\theta^* + 1/3 = -0.97 \pm 0.10$ and, thus, $\theta^* = -1.30 \pm 0.10$.

The numerical error in these estimates is relatively large and mainly arises from the numerical uncertainty for the value of the critical potential strength g_u . We estimated this error from a systematic variation of the critical potential strength g_u . Thus, we plotted each distribution for different values of g_u chosen from the interval $-0.396 \leq g_u \leq -0.400$ and estimated the critical exponents for each of these values. Within the numerical accuracy obtained in this way, all measured values for θ^* are compatible with the predicted value $\theta^* = -4/3$.

It is instructive to consider a somewhat different potential well which is only effective if the polymer enters the well (or defect) tangentially. In the presence of a hard wall, such a restriction for the attractive potential does

not change the polymer behavior since the semi-flexible polymer must touch the wall tangentially (otherwise, the curvature would be infinite). It seems plausible to expect that the same universality holds for the symmetric potential well considered here. This expectation is indeed confirmed by our numerical studies as described next.

Thus, we study the modified potential well

$$V(\ell, v) = V_{\delta\delta}(\ell, v) \equiv \begin{cases} \frac{g}{\Delta t}, & |\ell| \leq \ell_V \text{ and } |v| \leq \frac{\ell_V}{\Delta t}, \\ 0, & |\ell| > \ell_V \text{ or } |v| > \frac{\ell_V}{\Delta t}, \end{cases} \quad (29)$$

which is only effective if the polymer lies within the well and has an orientation which is (almost) parallel to this well.

In physical units, this corresponds to a potential well which has width z_V and strength u as given by equation (28) and for which the polymer only gains energy if its slope is sufficiently small and satisfies

$$\left| \frac{dz}{dt} \right| \leq \left(\frac{Tz_V}{\kappa} \right)^{1/3}. \quad (30)$$

For this modified potential, we could obtain the improved estimate $g_u = -0.468 \pm 0.001$ for the the critical attraction strength g_u using again the two methods described at the end of Section 3.2. We have now repeated the numerical analysis of the four different distribution functions as described above for the potential $V = V_{\delta}$. From the data for $P_{\text{tan}}^{(e)}(\ell)$, $P^{(e)}(\ell)$, $P_{\text{tan}}(\ell)$, and $P(\ell)$, we obtain $\theta^*/2 = -0.64 \pm 0.04$, $\theta^*/2 + 1/3 = -0.35 \pm 0.03$, $\theta^* = -1.29 \pm 0.08$, and $\theta^* + 1/3 = -0.98 \pm 0.08$, respectively. Again, all of these values are in reasonable agreement with the predicted value $\theta^* = -4/3$. Furthermore, these numerical results confirm the expectation that the modified, orientation-dependent potential wells $V = V_{\delta\delta}(\ell, v)$ belong to the same universality class as the usual potential wells $V = V_{\delta}(\ell)$.

3.4 Intermediate fluctuation regime

For directed lines or strings, *i.e.*, for one-dimensional objects which are governed by a line tension, a long-ranged potential can change the critical behavior [19]. This applies both to the unbound state and to the unbinding transition. The most interesting case is obtained in the so-called intermediate fluctuation regime [19,11]. In the latter case, the long-ranged interaction has a power law behavior which corresponds exactly to the behavior of the fluctuation-induced repulsion. Since such a long-ranged interaction is a marginal perturbation in the renormalization group sense the critical exponents depend continuously on the strength of this potential.

For a semi-flexible polymer, the relevant power law is $1/\ell^{2/3}$ [9,10]. Although the exact values of the critical exponents are not known, we can study the relation between the critical exponents x_0 and x^* for the unbound state and for the unbinding transition, respectively. This relation should still be given by $x^* + x_0 = 2$ as in (18).

For a hard wall and a long-ranged potential, the critical behavior has been studied numerically in [10]. Indeed, the conjecture expressed as equation (17) in [10], based only on numerical data, represents a special case of our general scaling relation (18) since the quantities α and β of reference [10] are identical with $\theta_0/2$ and $\theta^*/2$, respectively.

As shown in Section 3.1, the critical behavior at the delocalization transition in the absence of a hard wall differs from the behavior at the unbinding transition in the presence of such a wall. Thus, we expect that this distinction also applies to systems with a long-ranged potential which decays as $1/\ell^{2/3}$ for large ℓ . In exactly the same way as before, we can measure the exponents θ^* or x^* at the delocalization transition and determine their functional dependence on the strength of the long-ranged potentials. In order to regularize the divergence of the $\ell^{-2/3}$ power law at the origin, we use the potential

$$V(\ell) = \begin{cases} w\ell^{-2/3} & \text{for } |\ell| \geq \ell_V, \\ w(\Delta\ell)^{-2/3} + g & \text{for } |\ell| < \ell_V, \end{cases} \quad (31)$$

with $\ell_V = \Delta\ell$ as before where w parameterizes the strength of the long-ranged potential. We choose $g = 0$ in order to measure x_0 and θ_0 and study negative g in order to reach the delocalization transition at $g = g_u(w) < 0$. Since the critical exponents in the presence of a long-ranged potential are not known analytically we measure θ_0 or x_0 numerically as a function of the potential strength w . Inspection of Figure 3(a) shows that x_0 and x^* as measured in this way are quite symmetric with respect to $x = 1$ and, thus, fulfill the relation $x_0 + x^* = 2$ as in (18). As shown in Figure 3(a), a parabolic w -dependence given by

$$x_0(w) = 1 + \sqrt{1 - w/w_c} \quad \text{and} \quad x^*(w) = 1 - \sqrt{1 - w/w_c} \quad (32)$$

with $w_c \simeq -0.07$ represents a good fit to the numerically obtained values of the exponents. For directed lines or strings, such a parabolic w -dependence is an exact relation for all values of w . For $w < w_c$, the semi-flexible polymer is always bound, see Figure 3(b), and delocalization transitions occur only for $w > w_c$. As shown in Figure 3(b), the location of the transition line is described by the critical value g_u of the short-range attraction which varies with the strength w of the long-ranged potential.

4 Semi-flexible polymers in three dimensions

Two semi-flexible polymers without any interaction in a 3-dimensional system are described by the expression (4) with $d_{\perp} = 2$ from which we can immediately extract the exponent $x_0 = 4$. The general mapping discussed in Section 2 then implies that the delocalization transition induced in this system by a short-ranged attraction should belong to the same universality class as the transition of directed lines or strings in $1 + 8$ dimensions. The

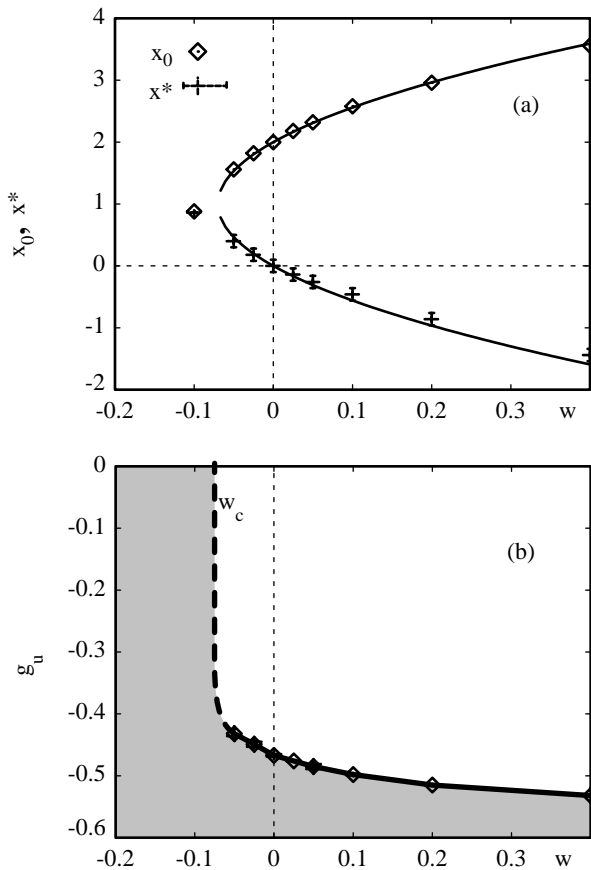


Fig. 3. Intermediate fluctuation regime. (a) Dependence of the critical exponent x on the strength w of the long-ranged potential. The solid lines correspond to the functions $1 \pm \sqrt{1 - w/w_c}$ with $w_c = -0.07$; and (b) Phase diagram of the delocalization transitions: The parameter g_u is the strength of the short-ranged potential at which the unbinding transition takes place. The shaded region corresponds to the bound state of the polymer.

latter transition is discontinuous but exhibits nontrivial scaling properties characterized by $\zeta_2^* = -2$ as follows from the results of reference [17]. The scaling relation $\theta^* = 2(x^* - 2d_\perp)/3 = 2(\zeta_2^* - 4)/3$ then leads to $\theta^* = -4$. Thus the probability distributions (14)–(17) should exhibit nontrivial power law behavior with $\theta^* = -4$. We will now present the results of numerical studies which are consistent with these scaling predictions.

In contrast to the situation in 1+1 dimensions, a transfer matrix approach is not feasible in 1 + 2 dimensions. Instead, we used Monte Carlo (MC) simulations in order to study the critical behavior. The semi-flexible polymer is discretized into L_\parallel segments of size Δt with periodic boundary conditions in the direction parallel to the polymer. The displacement of segment i is described by the continuous variable ℓ_i . The corresponding length scale $\Delta \ell$ was chosen to be $\Delta \ell \equiv (2T/\kappa)^{1/2}(\Delta t)^{3/2}$ which corresponds to the reduced bending stiffness $\kappa(\Delta \ell)^2/T(\Delta t)^3 = 2$. The excursions of the polymer in the perpendicular direction are confined to a cylinder of radius L_\perp . In the center of this cylinder, the polymer experiences an attrac-

tive potential well of strength g and of radius ℓ_V with $\ell_V = \Delta \ell/10$. Thus, the potential is given by

$$V(\ell, v) = V_{\text{cyl}}(\ell) \equiv \begin{cases} g, & |\ell| < \ell_V, \\ 0, & \ell_V \leq |\ell| \leq L_\perp, \\ \infty, & |\ell| > L_\perp. \end{cases} \quad (33)$$

In one MC step, each polymer segment undergoes a random perpendicular displacement. Such a displacement is accepted depending on the energy difference between the original and the displaced configuration according to the usual Metropolis rules. The maximal length of a trial displacement is chosen in such a way that a reasonable acceptance rate is achieved. The configurations are evaluated after an adjustable number of MC steps has been performed and the observables are averaged over many such measurements. The total number of MC steps and the number of steps between measurements are adjusted according to the system size and to the distance from the transition point in order to sample uncorrelated configurations. The maximal number of MC steps used was $2 \cdot 10^{10}$.

As expected, we find a delocalization transition at some critical value $g = g_u$ for the strength of the attractive potential well. One way to estimate this critical strength is via the dependence of the expectation value $\langle E \rangle$ of the total energy per polymer segment on the strength of the attractive well. As an example, we display the corresponding MC data for $L_\parallel = 200$ in Figure 4. Inspection of this figure shows that this quantity exhibits a jump at the transition point as expected for a first-order phase transition.

The first-order character can also be seen in Figure 5(a). This histogram shows, for $L_\parallel = 200$, the fraction of those polymer segments which are close to the potential well during the MC simulation for different depths g of the potential well. At $g = -4.25$, *i.e.*, slightly above the delocalization transition, essentially all segments are unbound. At $g = -4.35$, *i.e.*, below the delocalization transition, all configurations contain about 65 percent bound segments. For a second-order phase transition, the number of bound segments should increase continuously at the phase transition. In contrast, the histogram for $g = -4.3$ shows a bimodal distribution with two separate maxima. One maximum corresponds to configurations with almost no bound segments; the configurations, which represent the other maximum, also have of the order of 65 percent bound segments. Therefore, we observe the coexistence of the bound and the unbound state of the semi-flexible polymer.

As mentioned, we expect that the probability distribution $P(|\ell|)$ decays as a power law even though this phase transition is of first order. For periodic boundary conditions, the probability distribution $P(|\ell|)$ should behave as $P(|\ell|) \sim |\ell|^{\theta^* + 5/3}$. For $\theta^* = -4$, this leads to the theoretical prediction $P(|\ell|) \sim |\ell|^{-7/3}$. If we consider the distribution $P(|\ell|)$ slightly below the transition point, we indeed find a power law decay with $\theta_1 \equiv \theta^* + 5/3 \simeq -2.22$ as shown in Figure 5(b) for polymer length $L_\parallel = 800$. However, if the interaction strength g is too close to its critical

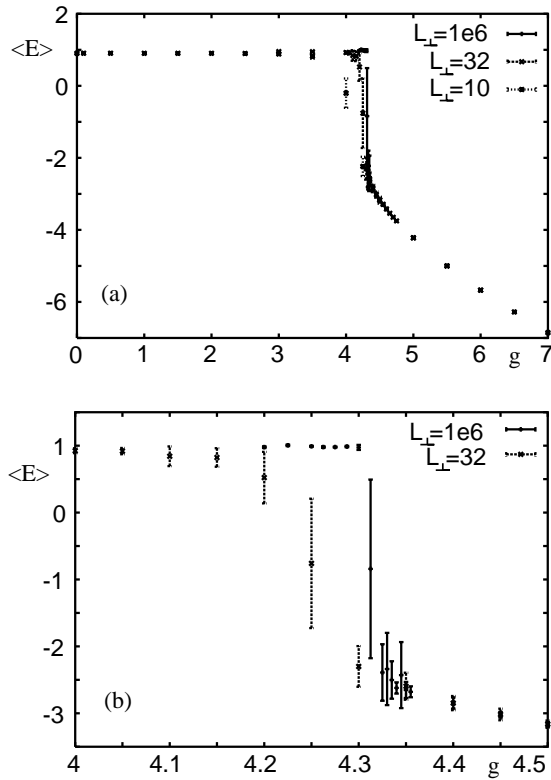


Fig. 4. Critical behavior in 1+2 dimensions. MC data for the dependence of the expectation value $\langle E \rangle$ of the total energy per polymer segment on the strength g of the attractive well. (a) The complete g -range studied in the simulations for different system sizes L_{\perp} at a fixed length $L_{\parallel} = 200$; and (b) A closer look at the g -values in the vicinity of the transition point.

value $g = g_u \simeq -4.3$ at the transition, this power law is obscured by exceptional fluctuations of the polymer from the bound to the unbound state. A good compromise seems to be the choice $g = -4.38$ as shown in Figure 5. This is still close enough to the phase transition so that the localization length which cuts off the power law still leaves a window of more than one order of magnitude to measure the power law behavior. This power law decay leads to the estimate $\theta_1 = -2.22 \pm 0.03$ for $g = -4.38$. However, as in 1+1 dimensions, the precise value of this exponent is found to depend on the strength g of the attractive well. Measuring again an effective exponent $\theta_1(g)$ in the vicinity of $g_u \simeq -4.3$, we get the estimate $\theta_1 = -2.2 \pm 0.2$. Therefore the numerical data are consistent with the prediction $P(|\ell|) \sim |\ell|^{-7/3}$.

We also measured the distribution $P_{\text{tan}}(|\ell|)$ of tangentially oriented segments which should scale as $P_{\text{tan}}(|\ell|) \sim |\ell|^{\theta^*+1}$. For the latter quantity, we find a power law with exponent $\theta^* + 1 \approx -2.7 \pm 0.25$, where the error is again estimated from the variation of the measured effective exponent with the potential strength g in the vicinity of $g_u \simeq -4.3$. This is again consistent with the theoretically predicted value $\theta^* = -4$.

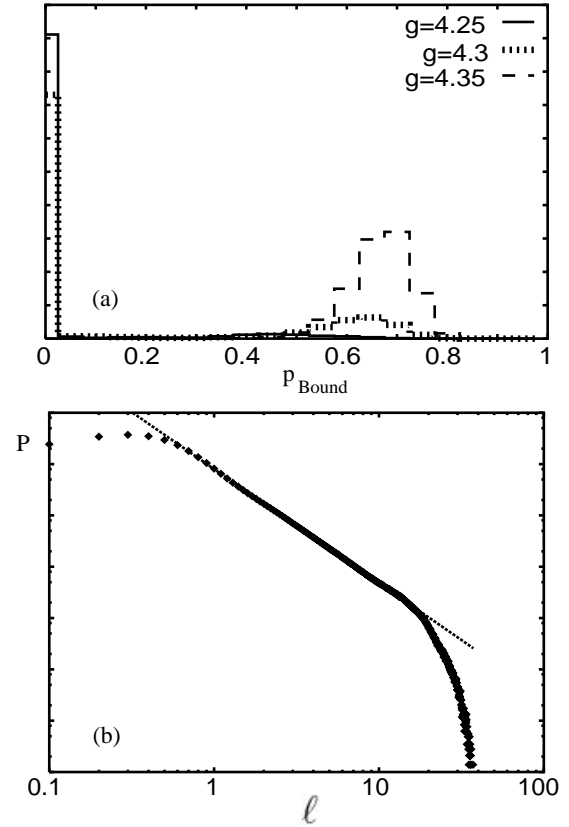


Fig. 5. Critical behavior in 1+2 dimensions. (a) Histogram of the fraction of bound segments. The two maxima correspond to configurations without bound segments and with approximately 65 percent bound segments, respectively. The different behavior at the three different g -values is explained in the text; and (b) Double logarithmic plot of the probability distribution $P(|\ell|)$ for finding a polymer segment at distance $|\ell|$ for attractive potential strength $g = -4.38$ and polymer length $L_{\parallel} = 800$. The line corresponds to the power law decay $\ell^{\theta^*+5/3}$ with $\theta^* + 5/3 = -2.22$.

5 Conclusion and outlook

In summary, we have systematically studied unbinding and delocalization transitions of semi-flexible polymers in the presence of short-ranged interactions. In 1+1 dimensions, four different universality classes must be distinguished governed by four different fixed points which correspond i) to a free semi-flexible polymer, ii) to a semi-flexible polymer in the presence of an attractive potential well, iii) to a semi-flexible polymer in the presence of a hard wall, and iv) to a semi-flexible polymer in the presence of both a hard wall and an attractive well. In all four cases, a combination of scaling arguments, transfer matrix calculations, and field-theoretic perturbation theory leads to definite theoretic predictions for the critical exponents which have been confirmed numerically. In 1+2 dimensions, the delocalization transition was shown to be strongly first order. Nevertheless, the probability distributions close to the transition point were found to decay with characteristic power laws.

In real systems, one often has *bundles* of many semi-flexible polymers which are bound together by attractive interactions. Examples are provided by bundles of actin filaments or by simplexes of semi-flexible polyelectrolytes. The size of these bundles is also governed by the competition between attractive interactions and fluctuation-induced repulsions of entropic origin. Therefore, such bundles also undergo unbinding transitions as one varies a control parameter such as, *e.g.*, the temperature. A systematic study of these transitions remains to be done.

We thank C. Hiergeist and T. Hwa for useful discussions, and J. Kierfeld for a critical reading of the manuscript.

Appendix A. Field-theoretic approach to unbinding transitions

In this appendix we want to give a brief explanation of the mapping between the field theory for a semi-flexible polymer with short range interactions and the field theory for a directed line or string with similar interactions. As explained in Section 2.3, this mapping allows the derivation of the relations (18) and (19) for semi-flexible polymers by translating the corresponding results as obtained in [17] for directed lines.

A semi-flexible polymer subject to a short-ranged attraction is described by the energy functional

$$\bar{\mathcal{H}}[\ell] = \bar{\mathcal{H}}_0[\ell] + g_0 \int_0^{L_{||}} \Phi_0(t)[\ell] dt, \quad (\text{A.1})$$

with the interaction operator

$$\Phi_0(t)[\ell] = \delta(\ell(t)). \quad (\text{A.2})$$

Due to the fact, that the semi-flexible polymer is stiff, an interaction can in principle depend on the local orientation of the polymer in an arbitrary way. It turns out that the interaction relevant for the unbinding transition is described by the local field

$$\Pi_0(t)[\ell] \equiv \delta(\ell(t)) \delta\left(\frac{d\ell(t)}{dt}\right) \quad (\text{A.3})$$

acting only if the polymers touch tangentially [16]. This kind of interaction stems from the fact that a semi-flexible polymer which crosses the potential well in several points not too far away from each other is forced by its own stiffness to stay tangential to the potential well. So any noticeable (multi contact) interaction with the potential well can only come from configurations where the polymer is tangential to the well. This is exactly what the additional factor $\delta(d\ell/dt(t))$ in the interaction operator Π_0 describes. So we replace Φ_0 by Π_0 in (A.1) and work with the energy functional

$$\bar{\mathcal{H}}[\ell] = \bar{\mathcal{H}}_0[\ell] + h_0 \int_0^{L_{||}} \Pi_0(t)[\ell] dt. \quad (\text{A.4})$$

A perturbative expansion of, *e.g.*, the free energy of this problem will be a series in h_0 with the coefficients expressed as integrals over expectation values of the form $\langle \Pi_0(t_1) \Pi_0(t_2) \dots \Pi_0(t_n) \rangle_0$. The expectation values have to be taken with respect to the free system at $h_0 = 0$. Since the polymer is one-dimensional we can always assume that the “times” t_1, t_2, \dots , are ordered which makes calculating this expectation value very easy. Using the Markov property of the path integral we simply get the product

$$\begin{aligned} & \langle \Pi_0(t_1) \Pi_0(t_2) \dots \Pi_0(t_n) \rangle_0 \\ &= \langle \Pi_0(0) \rangle_0 Z_{0,t_2-t_1}(0,0|0,0) \dots Z_{0,t_n-t_{n-1}}(0,0|0,0), \end{aligned} \quad (\text{A.5})$$

over several of the propagators of the free system.

Now imagine doing the same operations for directed lines. A free directed line is described by the energy functional

$$\bar{\mathcal{H}}_0^{\text{DP}}[\ell] \equiv \int_0^{L_{||}} \frac{1}{2} \left(\frac{d\ell}{dt} \right)^2 dt$$

and its unbinding transitions are described by

$$\bar{\mathcal{H}}^{\text{DP}}[\ell] = \bar{\mathcal{H}}_0^{\text{DP}}[\ell] + g \int_0^{L_{||}} \delta(\ell(t)) dt. \quad (\text{A.6})$$

Since the typical path of a directed line does not have a well-defined slope its partition function (or propagator) is already fixed by prescribing the starting and end position $\ell(0) = \ell_0$ and $\ell(L_{||}) = \ell_1$. It is defined by the path integral

$$Z_{L_{||}}^{\text{DP}}(\ell_1|\ell_0) = \int \mathcal{D}\ell \exp\left(-\bar{\mathcal{H}}_0^{\text{DP}}[\ell]\right).$$

Evaluating this path integral gives for a d'_{\perp} -dimensional displacement field $\ell(t)$

$$Z_{L_{||}}^{\text{DP}}(\ell_1|\ell_0) = \left(\frac{1}{2\pi L_{||}} \right)^{d'_{\perp}/2} \exp\left[-\frac{(\ell_1 - \ell_0)^2}{2L_{||}}\right]. \quad (\text{A.7})$$

Calculating the perturbation expansion of (A.6) will obviously give exactly the same series as the perturbation expansion of (A.4) except that each expectation value $\langle \Pi_0(t_1) \Pi_0(t_2) \dots \Pi_0(t_n) \rangle_0$ is replaced by $\langle \delta(\ell(t_1)) \dots \delta(\ell(t_n)) \rangle_0^{\text{DP}}$. For the directed line these expectation values also factorize giving

$$\begin{aligned} & \langle \delta(\ell(t_1)) \dots \delta(\ell(t_n)) \rangle_0^{\text{DP}} = \\ & \langle \delta(\ell(0)) \rangle_0^{\text{DP}} Z_{0,t_2-t_1}^{\text{DP}}(0|0) \dots Z_{0,t_n-t_{n-1}}^{\text{DP}}(0|0). \end{aligned}$$

Comparing this with (A.5) we conclude that except for the uninteresting global prefactor $\langle \Pi_0(0) \rangle_0$ or $\langle \delta(\ell(0)) \rangle_0^{\text{DP}}$ the only difference between the perturbation theory describing the unbinding transition of a semi-flexible polymer and the perturbation theory describing the unbinding transition of a directed line is the replacement of $Z_{0,t}^{\text{DP}}(0|0)$ by $Z_{0,t}(0,0|0,0)$.

Looking at (10) we conclude that $Z_{0,t}(0,0|0,0) \sim t^{-x}$ whereas (A.7) gives us $Z_{0,t}^{\text{DP}}(0|0) \sim t^{-d'_{\perp}/2}$. So up to a number which always can be absorbed into the definition

of the coupling constants the perturbation series for the unbinding transition of the semi-flexible polymer characterized by the exponent x is term by term the same as the perturbation series of directed lines in $d'_\perp = 2x$ dimensions. We therefore conclude that the phase transitions of these two systems are equivalent. In particular, for semi-flexible polymers with mutual attractions and no other constraints like a hard wall, we get from (4) $x = 2d_\perp$. Therefore the unbinding transition for free semi-flexible polymers in $1 + d_\perp$ dimensions is equivalent to the unbinding transition of directed lines in $1 + 4d_\perp$ dimensions.

References

1. See, e.g., B. Alberts, *et al.*, *Molecular Biology of the Cell* (Garland Publ., New York, 1983).
2. P.-G. de Gennes, *Scaling Concepts in Polymer Physics* (Cornell University Press, Ithaca & London, 1979).
3. O. Kratky, G. Porod, *Rec. Trav. Chim.* **68**, 1106 (1949).
4. R.A. Harris, J.E. Hearst, *J. Chem. Phys.* **44**, 2515 (1966).
5. N. Saito, K. Takahashi, Y. Yunoki, *J. Phys. Soc. Jpn.* **22**, 219 (1967).
6. T. Odijk, *J. Polymer Sci.* **15**, 477 (1977).
7. J. Skolnick, M. Fixman, *Macromolecules* **10**, 944 (1977).
8. A.C. Maggs, D.A. Huse, S. Leibler, *Europhys. Lett.* **8**, 615 (1989).
9. R. Lipowsky, *Phys. Rev. Lett.* **62**, 704 (1989).
10. G. Gompper, T.W. Burkhardt, *Phys. Rev. A* **40**, 6124 (1989).
11. For a review, see R. Lipowsky, *Phys. Scr. T* **29**, 259 (1989).
12. J. Käs, H. Strey, M. Bärmann, E. Sackmann, *Europhys. Lett.* **21**, 865 (1993).
13. A. Ott, M. Magnasco, A. Simon, A. Libchaber, *Phys. Rev. E* **48**, 1642 (1993).
14. E. Frey, K. Kroy, J. Wilhelm, E. Sackmann, in *Proceedings of Les Houches Workshop on "Networks in Physics and Biology"*, Les Houches (France), 16-21 March 1997 (Editions de Physique, Springer Verlag, 2000).
15. R. Bundschuh, PhD Thesis, Universität Potsdam (1996).
16. R. Bundschuh, M. Lässig, preprint (1999).
17. R. Lipowsky, *Europhys. Lett.* **15**, 703 (1991).
18. T.W. Burkhardt, *J. Phys. A* **26**, 1157 (1993).
19. R. Lipowsky, T. Nieuwenhuizen, *J. Phys. A: Math. Gen.* **21**, L89 (1988); S. Grothans, R. Lipowsky, *Phys. Rev. A* **45**, 8644 (1992).
20. C. Hiergeist, Diploma Thesis, Universität zu Köln (1994).
21. C. Hiergeist, M. Lässig, R. Lipowsky, *Europhys. Lett.* **28**, 103 (1994).
22. L. Balents, M. Kardar, *Europhys. Lett.* **23**, 503 (1993).
23. T. Hwa, T. Nattermann, *Phys. Rev. B* **51**, 455 (1995).
24. H. Kinzelbach, M. Lässig, *J. Phys. A: Math. Gen.* **28**, 6535 (1995); *Phys. Rev. Lett.* **75**, 2208 (1995).
25. K. Willbrand, Diploma Thesis, Technische Hochschule Aachen (1996).
26. For a review, see M. Lässig, *J. Phys. C* **10**, 9905 (1998).